Power Management of an off-grid hybrid PV-Wind-Battery System including electrical and hydraulic loads

Malek Zaibi, Gérard Champenois, Xavier Roboam, Jamel Belhadj, Bruno Sareni

POWER MANAGEMENT OF A OFF-GRID Y RID PV-WIND-ATTERY SYSTEM INCLUDING ELECTRICAL AND YDRAULIC LOADS

M. Zaibi [1, 2], G. Champenois[1], X. Roboam[3], J. Belhadj[2], B. Sareni[3]

1. LIAS, Université de Poitiers, ENSIP B25 2 rue Pierre Brousse BP 633, 86022 Poitiers, France.
2. LSE, Université de Tunis El Manar, ENIT BP 37, 1002 Tunis Le Belvédère, Tunisie
3. LAPLACE, Université de Toulouse, ENSEEIHT, 2 Rue Camichel 31071 Toulouse Cedex, France
e-mail: malek.zaibi@univ-poitiers.fr

Abstract – In this paper a hybrid photovoltaic (PV)/wind/battery system for off-grid applications with its Power Management System (PMS) is investigated. The Hybrid PV-wind is coupled via converters to battery stack for electrical storage and Motor-pumps for water production and hydraulic storage. The global power management strategy is defined for sharing the power flows between the battery and the hydraulic loads taking the irradiation and the wind speed into account. The hybrid system with its PMS is developed and tested using a dynamic simulator. The system performance is shown under different scenarios and operation modes. Several tests are carried out using real meteorological data of a remote area and a practical load demand profile.

Keywords – Hybrid system, battery storage, hydraulic system, dynamic simulator, power management.

1. INTRODUCTION

Off-grid power supply systems based on renewable energies are of great interest for applications such as remote areas electrification, telecommunication stations powering, water pumping and/or desalination for irrigation or drinking. These systems usually exploit the coupling between photovoltaic (PV) and wind generators but can also be coupled to conventional generators such as Diesel generator [1], fuel cells [2]-[3], micro-hydro generators [4] and batteries [2]-[5]. In this paper, a hybrid off-grid supply system including PV and wind generators with battery storage is studied for producing electricity and water from pumping and desalination. In such device, the use of a Power Management System (PMS) is of prime importance for optimal operation and constitutes a key feature. The rest of the paper is organized as follows. In section 2, the system configuration is defined and system components models employed for each subsystem are briefly described. Section 3 is devoted to the power management strategy aiming at optimizing the power and water flows. Section 4 reports the simulation results and the analysis of the system performance under various scenarios. Finally, conclusions are drawn in section 5.

2. SYSTEM CONFIGURATION

The Fig. 1 shows the configuration of a hybrid PV/WT generator coupled with two kinds of storage i.e. electric (battery) and hydraulic (tank).

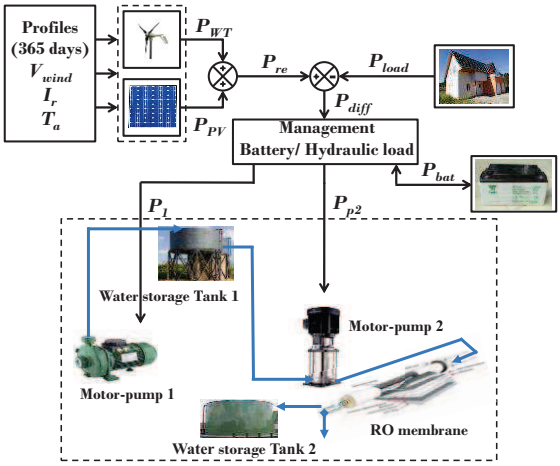

Fig. 1. Global system architecture

The meteorological profiles: wind speed (V_{wind}), solar irradiation (I_r) and ambient temperature (T_a) of a typical region in Tunisia have been recorded during one year. The power flows of the hybrid PV/WT source is shared between electrical and/or hydraulic loads and both kinds of storage (battery and tanks). A dynamic simulator has been developed using MATLAB/Simulink® environment. In this dynamic simulator, six subsystems are implemented: the PV generator, the wind turbine, the battery storage, the electrical load, the hydraulic load and the PMS.

2.1. HYBRİD ENERGY SOURCE MODELS

2.1.1. PV GENERATOR MODEL

The power PV generator is determined from [5]:

$$P_{PV} = \eta_r \eta_{pc}[1 - \beta(T_c - NOCT)]A_{PV}I_r \quad (1)$$

where η_r is PV efficiency, η_{pc} the power tracking equipment efficiency, which is equal to 0.9 with a perfect maximum point tracker, β the temperature coefficient, ranging from 0.004 to 0.006 per °C for silicon cells, *NOCT* is normal operating PV cell temperature (°C), A_{pv} the PV panels area (m^2) and T_c the PV cell temperature (°C) which can be expressed by (2).

$$T_c = 30 + 0.0175(I_r - 300) + 1.14(T_a - 25) \quad (2)$$

where T_a denotes the ambient temperature (°C).

2.1.2. WİND TURBİNE MODEL

The wind turbine power is expressed as follows [5]:

$$P_{wt} = \frac{1}{2} C_p \rho A_{wt} {V_{wind}}^3 \quad (3)$$

where C_p is the wind turbine efficiency, ρ the air mass density and A_{wt} the wind turbine swept area.

2.1.3. BATTERY STORAGE MODEL

In this study, we propose an ideal model for the battery. During the charging and discharging process, the state of charge (SOC) vs time (t) can be described by [5]:

$$SOC(t) = \begin{cases} SOC(t - \Delta t) + P_{Bat} \frac{\eta_{ch}}{U_{bus}} \Delta t \\ SOC(t - \Delta t) + P_{Bat} \frac{1}{\eta_{dis} U_{bus}} \Delta t \end{cases} \quad (4)$$

where Δt is the time step (here, half an hour), P_{Bat} represents the battery power determined by the PMS, η_{ch} and η_{dis} are respectively the battery efficiencies during charging and discharging phase. U_{bus} denotes the nominal DC bus voltage.

At any step time Δt, the SOC must comply with the following constraints:

$$SOC_{in} \leq SOC(t) \leq SOC_{ax} \quad (5)$$

where SOC_{in} and SOC_{ax} are maximum and minimum allowable storage capacities, respectively.

2.1.4. ELECTRİCAL LOAD PROFİLE

Typical power consumption data P_{load} were acquired for a residential home. During 365 days with an half an hour acquisition period, this profile describes a weekday and weekend day consumption.

2.2. HYDRAULİC LOAD MODELS

The hydraulic load system is shown in Fig. 1. It includes four principal subsystems: the motor-pump 1, water storage tank 1, the motor-pump 2 with reverse osmosis and tank water storage 2.

2.2.1. MODEL OF THE MOTOR-PUMP 1

The motor-pump model CRN-3-10 of GRUNDFOS nominal power has been selected for pumping water from well to the tank water storage 1. The rated motor-pump power is 0.75 kW. The characteristics $H(Q_1)$ and the efficiency curve of the motor-pump 1 for two frequencies 50 Hz and 40 Hz and the load characteristic $H_{load}(Q_1)$ are shown in Fig. 2.

The operating point of pumping is the crossing point between $H(Q_1)$ and $H_{load}(Q_1)$. A weak variation of the motor-pump frequency (i.e. 40 Hz) decreases the pump efficiency. For this reason, we use the optimal operation of pump 1 with a fixed frequency (i.e. 50Hz).

The electric power P_1 required to motor-pump 1 at head H and flow rate Q_1 can be calculated as:

$$P_1 = \frac{\rho_w g H Q_1}{\eta_m \eta_p} \quad (6)$$

where ρ_w is the density of water (kg/m^3), g the gravity constant (m/s^2), η the motor efficiency and η_p the pump efficiency.

2.2.2. MODEL OF THE WATER STORAGE TANK 1

The water tank 1 is used to store brackish water. It is characterized by its water level L_1 and its section S_1. The level L_1 can be calculated as:

$$L_1(t) = L_1(t - \Delta t) + \frac{Q_1(t) - Q_2(t)}{S_1} \Delta t \quad (7)$$

This tank is instrumented with four sensors measuring four different water levels: two minimum sublevels, i.e. high and low (L^1_{minH} and L^1_{minL}) and two maximum sublevels, i.e high and low (L^1_{maxH} and L^1_{maxL}). The high and low levels are separated by a hysteresis band. This hysteresis avoids the switch on/off of motor-pump during operation.

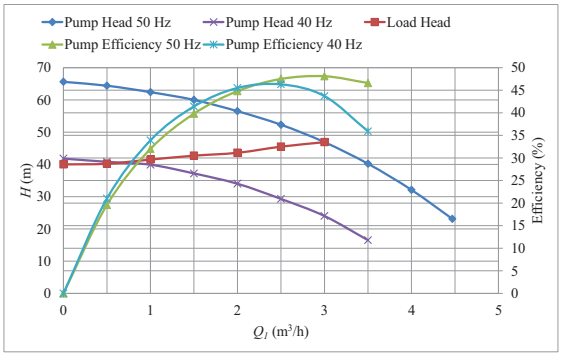

Fig. 2. Hydraulic Characteristic Motor-pump 1

2.2.3. MODEL OF THE MOTOR-PUMP 2

The motor-pump model CRN-3-29 of GRUNDFOS has been selected for water pumping from the tank water storage 1 to the tank water storage 2 via reverse osmosis (RO) desalination system. The rated motor-pump power is 2.2 kW.

Contrary to the case of the motor-pump 1, the motor-pump can operate with variable frequency keeping a good efficiency (see fig.4). It is interesting to match the energy availability with the power of the pump 2 for maximizing the water production. The pump head pressure must be greater than the osmotic pressure.

Fig. 3 presents three characteristics $H(Q_2)$ with the efficiency curves of the motor-pump 2 for the corresponding frequencies: 50 Hz, 38 Hz and 27 Hz, and also the load characteristic $H_{load}(Q_2)$.

By satisfying the previous constraints, the motor-pump 2 frequency varies between 50 Hz and 27 Hz.

The expression of the flow rate Q_2 is function of the electric power P_{P2}.

$$Q_2 = -2{,}17.10^{-7}P_{P2}^2 + 10{,}7.10^{-4}P_{P2} + 0{,}683 \quad (8)$$

P_{P2} corresponds with the electric power required to the motor-pump 2 at every duty points from 27 Hz to 50 Hz.

For the RO process, the flow rate Q_2 is separated between the permeate flow Q_{2a} and the concentrate flow Q_{2b}. This two flows are function of the pressure P_2 and are defined as follows [6] :

$$\begin{cases} P_2 = (R_{valve} + R_{odule})Q_{2b}^2 \\ Q_{2a} = \frac{P_2}{R_{membrane}} \\ Q_2 = Q_{2a} + Q_{2b} \end{cases} \quad (9)$$

where $R_{membrane}$, R_{module} and R_{valve} are the hydraulic resistances of the membrane, the module and the valve, respectively.

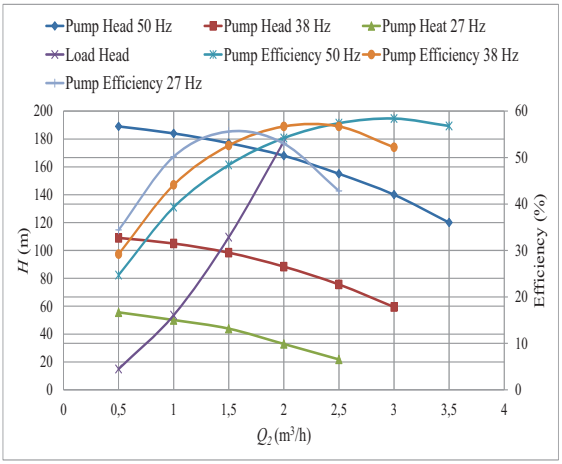

Fig. 3. Hydraulic Characteristic Motor-pump 2

2.2.4. MODELİNG OF THE FRESH WATER STORAGE TANK 2

The water storage tank 2 is the tank of permeate (fresh) water. It is characterized by the level L_2 and section S_2. The level L_2 can be calculated as:

$$L_2(t) = L_2(t-\Delta t) + \frac{Q_{2a}(t) - Q_{load}(t)}{S_2}\Delta t \quad (10)$$

where Q_{load} is the water flow demand required by the consumers.

A previously, this tank is instrumented by four level sensors: two useful levels, i.e. high and low (L^2_{uH} and L^2_{uL}) and two maximum levels, i.e. high and low (L^2_{maxH} and L^2_{maxL}). The high and low levels are also determined by a hysteresis band.

3. POWER MANAGEMENT STRATEGY

The strategy of the proposed power management is presented in Fig. 4. The primary objectives of power management are as follows:

1. Minimize the Loss of electric Power Supply Probability ($LPSP^E$),
2. Maximize water production and minimize the Loss of hydraulic Power Supply Probability $LPSP^H$,
3. Maximize the battery life by controlling the state of charge (SOC)

The input of the power management is the difference power P_{Diff}. P_{Diff} corresponds with the remaining power calculated by the difference between the source power (P_{wt}+P_{PV}) and the load electric power P_{load}. This power is obtained at each computation step by the dynamic simulator taking account of the wind speed, the solar irradiation, the ambient temperature and the load electric power.

The power management strategy depends on the magnitude of P_{Diff}, the SOC and the levels of the tank 1 and 2. Seven scenarios are possible and explained below and grouped in Fig. 5.

First: P_{Diff} negative

- Scenario (a): ($P_{Diff} < 0$)

If the SOC is greater than SOC_{min} then the battery discharges at P_{Diff} because $P_{bat} = P_{Diff}$

If the SOC is smaller than SOC_{min} then the production cannot be satisfied and the $LPSP^E$ increases with P_{Diff}. The $LPSP^E$ is calculated by:

$$LPSP^E(\%) = \frac{\sum_{\Delta t=1}^{T} |P_{Diff}(\Delta t)|\Delta t}{\sum_{\Delta t=1}^{T} P_{load}(\Delta t)\Delta t} \quad (11)$$

Note in this scenario that zero power is sent towards the hydraulic system

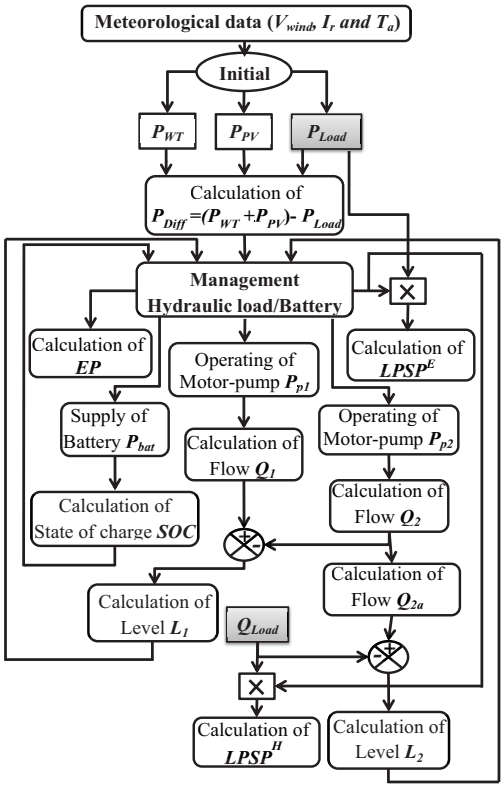

Fig. 4. Flowchart of the proposed power management strategy.

Second: P_{Diff} positive

For all the following scenarios, if battery *SOC* is less than the "useful state of charge" SOC_u, then P_{Diff} is used to charge the battery: $P_{bat} = P_{Diff}$. SOC_u is a typical level of the *SOC* than gives the preference to store P_{Diff} in the battery instead of using it for the hydraulic load. This strategy then aims at minimizing the $LPSP^E$ criterion while limiting the depth of discharge (*DOD*) for maximizing battery life.

➢ Scenario (b): ($0 < P_{Diff} < P_{2\ in}$)

If the *SOC* is smaller than SOC_{max} then the power P_{Diff} is stored in the battery and $P_{bat} = P_{Diff}$.

If the *SOC* is greater than SOC_{max}, then the battery is full and P_{Diff} is lost. In this case, a coefficient of excess of production *EP* is returned. This coefficient is computed from the excess power ($P_{Excess} = P_{Diff}$) as follows:

$$EP(\%) = \frac{\sum_{\Delta t=1}^{T} P_{Excess}(\Delta t)\Delta t}{\sum_{\Delta t=1}^{T} P_{load}(\Delta t)\Delta t} \quad (12)$$

For all the following scenarios, when the battery is full ($SOC>SOC_{max}$) the same conditions are met.

Similarly, if the tank 2 is empty ($L_2 < 0$) the loss of hydraulic power supply probability $LPSP^H$ is calculated as:

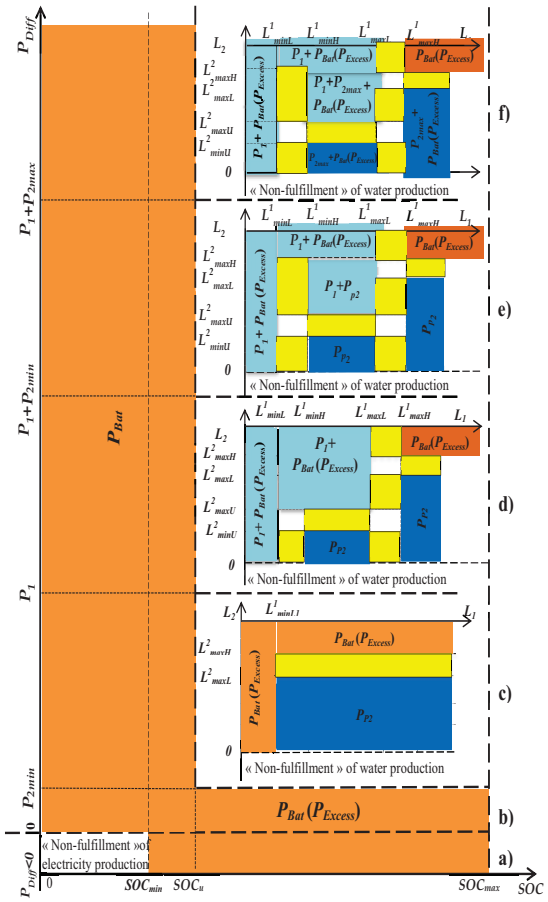

Fig. 5. Proposed power management strategy for hybrid PV/Wind/Battery system.

$$LPSP^H(\%) = \frac{\sum_{\Delta t=1}^{T} Q_{load}(\Delta t)\Delta t}{Q_{load}T} \quad (13)$$

➢ Scenario (c): ($P_{2\ in} < P_{Diff} < P_1$)

If the tank 1 is empty ($L_1 < L^1_{minL}$) or if the tank 2 is full ($L_2 > L^2_{maxH}$), the pump 2 cannot operate. In this case, P_{Diff} is stored in the battery or P_{Excess} is increased if the battery is full.

In all other conditions: pumping mode for pump 2 is active; P_{P2} (P_{P2}: pump 2 electric power) follows P_{Diff}. The level 2 (tank 2) depends on the pump 2 water flow and on the water used (Q_{load}). So, it is possible that the tank reach its maximum level. In this case for preventing the switching between the power P_{P2} and the power P_{Bat}, an hysteresis band on the level 2 [L^2_{maxL}, L^2_{maxH}] has to be defined (in yellow on the Fig. 5). Inside the hysteresis band, the algorithm is as follows:

$$if\ P_{P2}(t-\Delta t) = P_{Diff}(t-\Delta t)$$
$$then \begin{cases} P_{P2}(t) = P_{Diff}(t) \\ P_{Bat}(t) = 0 \end{cases} \quad (14)$$

$$if\ P_{Bat}(t-\Delta t) = P_{Diff}(t-\Delta t)$$
$$then \begin{cases} P_{Bat}(t) = P_{Diff}(t) \\ P_{P2}(t) = 0 \end{cases} \quad (15)$$

Scenario (d): ($P_1 < P_{Diff} < P_1 + P_{2\ in}$)

If tank 2 is empty or lower than a usage level L^2_U and the tank 1 is not empty then P_{Diff} is used for the pump 2 ($P_{p2} = P_{Diff}$). The usage level L^2_U is chosen to favor the fresh water availability, so as to minimize the $LPSP^H$ criterion. On the contrary, if tank 1 is empty or tank 2 is higher than the usage level L^2_U then P_{Diff} is shared between P_1 and P_{Bat} (P_1+P_{Bat}= P_{Diff}) or P_{Excess} (P_1+ P_{Excess} = P_{Diff}) if the battery is full.

If both tank 1 and tank 2 are full, the power P_{Bat} is equal to P_{Diff} or P_{Diff} =P_{Excess} if the battery is full.

In this scenario, four hysteresis bands are defined. They are descripted as follows (in yellow on the Fig. 5):

- Three hysteresis band in the minimum tank level 1 [L^1_{minL}:L^1_{minH}], the minimum tank level 2 [L^2_{minU}:L^2_{maxU}] and the maximum tank level 1 [L^1_{maxL}:L^1_{maxH}] for eliminating the switching between the powers P_{P2}, P_1 and P_{Bat} or P_{Excess} if the battery is full.
- Hysteresis band in the maximum tank level 2 [L^2_{maxL}:L^2_{maxH}] is previously described in scenario (c)

➢ Scenario (e): ($P_1 + P_{2\ in} < P_{Diff} < P_{2\ ax}$)

In this scenario, it is possible to share P_{Diff} between the power P_1 and the power P_{P2} (P_1+P_{Pp2} = P_{Diff}). This occurs when the tank level 1 is not full and when the level of the tank 2 is between L^2_U and L^2_{max}.

In all other conditions, the scenario is the same as the scenario (d).

➢ Scenario (f): ($P_{Diff} > P_1 + P_{2\ ax}$)

This scenario is similar to scenario (e), except for all power P_{P2} are replaced by P_{2max}+P_{Bat} or P_{2max}+ P_{Excess} if the battery is full.

4. Results Analysis

Table I. Simulation parameters

SOC_{ini}	SOC_{min}	SOC_u	SOC_{max}	L^1_{ini}	L^1_{minL}
80 %	30 %	60 %	100 %	2 m	0.1m
L^1_{minH}	L^1_{maxL}	L^1_{maxH}	P_1	P_{2min}	P_{2max}
0.3 m	1.9 m	2 m	796 W	314 W	1863 W
L^2_{ini}	L^2_{minU}	L^2_{maxU}	L^2_{maxL}	L^2_{maxH}	
2 m	0.4 m	0.6 m	1.9 m	2 m	

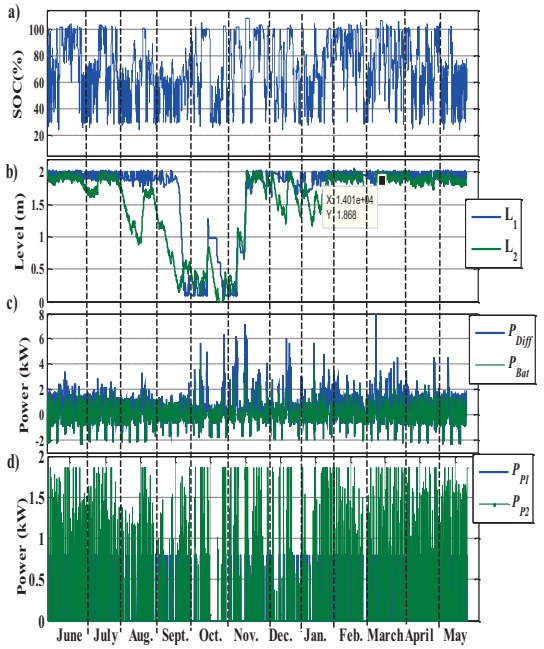

Fig. 6.Evolution of (a) battery *SOC*, (b) tank levels (1,2), (c) battery power and difference Power, (d) absorbed powers on pumps (1,2) as a function of time

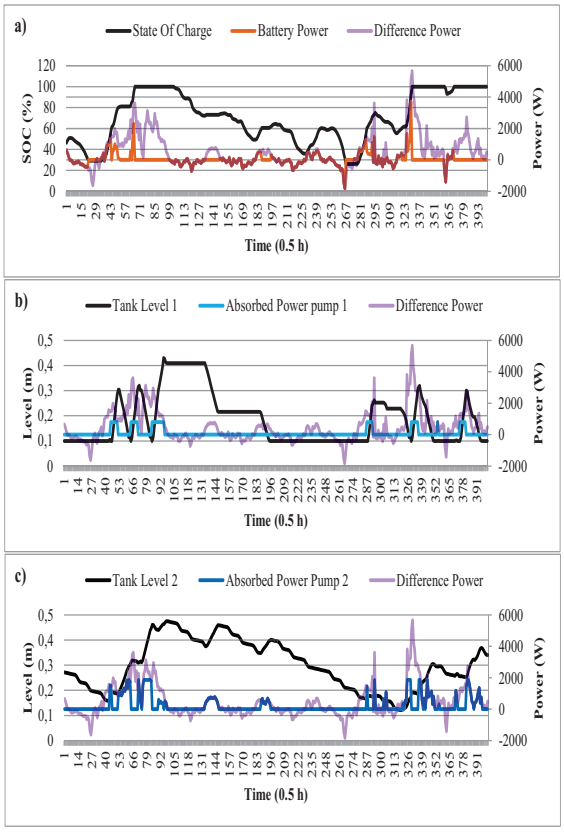

Fig. 7. Profile vs. time (during 200 hours) of: (a) battery *SOC* and P_{Bat}, (b) level of tank 1 and absorbed power on pump 1, (c) level of tank 2 and absorbed power on pump 2, (a, b, c) difference power (P_{diff}).

Using the dynamic simulator with the system parameters of Table I, simulations were carried out in order to validate the PMS performance under different scenarios.

Fig. 6 shows the results of the battery state of charge (*SOC*), the tank levels (L_1 and L_2), the battery power (P_{Bat}), the difference power (P_{Diff}) and the power absorbed on both pumps (P_1 and P_{P2}) vs time (for a half-hourly sampling).

Table II shows the results of the system indicators: the loss of electric and hydraulic Power Supply Probability and the excess of production.

Table II. Results of system indicators

$LPSP^E$	$LPSP^H$	*EP*
6.145 %	0.865 %	20,48 %

To better see the details, a zoom during 200 hours in October is shown in Fig. 7. In this figure, different scenarios can be identified at the following time intervals in Fig. 8.

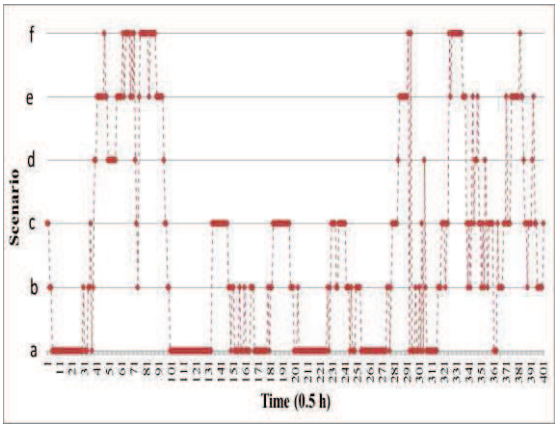

Fig. 8. Scenarios vs. time (during 200 hours)

5. Conclusion

In this paper, an off-grid hybrid PV/wind/battery system is proposed for water pumping and desalination. The system configuration, the system components models and the global power management strategy for the hybrid energy system is presented. The dynamic simulator has been developed using MATLAB/Simulink. Simulation studies have been carried out to validate the system performance under various scenarios with the real meteorological data and the typical load demand of a residential home. The results show the effectiveness of the overall power management energy and the feasibility of the proposed hybrid energy system. In the next studies, an optimal design of this hybrid system will be investigated.

Acknowledgements

The authors acknowledge the CMCU UTIQUE Program for financial support. This work was supported by the Tunisian Ministry of High Education and Research under Grant LSE-ENIT-LR 11ES15.

References

[1] SM. Shaahid and I. El-Amin, Techno-economic evaluation of off-grid hybrid photovoltaic–diesel–battery power systems for rural electrification in Saudi Arabia—a way forward for sustainable development, Renewable & Sustainable Energy Reviews, Volume 13, Issue 3, pp 625–633, 2009.

[2] D. Ipsakisa, S. Voutetakis, P. Seferlis, F. Stergiopoulos and C. Elmasides, Power management strategies for a stand-alone power system using renewable energy sources and hydrogen storage, Inter. Journal of Hydrogen Energy, Volume 34, Issue 16, pp 7081–7095, 2009.

[3] C. Wang and M. H. Nehrir, Power Management of a Stand-Alone Wind/Photovoltaic/Fuel Cell Energy System, IEEE Trans. On Energy Conversion, Volume:23 , Issue 3, pp 7081-7095, 2008.

[4] C. Bueno and JA. Carta, Wind powered pumped hydro storage systems, a means of increasing the penetration of renewable energy in the Canary Islands, Renewable and Sustainable Energy Reviews, Volume 10, Issue 4, pp 312–340, 2006

[5] D. Abbes, A. Martinez and G. Champenois, "Life cycle cost, embodied energy and loss of power supply probability for the optimal design of hybrid power systems", Math. Comput. Simul, http://dx.doi.org/10.1016/j.matcom.2013.05. 004, 2013.

[6] M. Turki, J. Belhadj and X. Roboam, "Control strategy of an autonomous desalination unit fed by PV-Wind hybrid system without battery storage", J. Electrical Systems, 4-2,pp 1-12, 2008